Spherulitic crystallization in poly(bis(trifluoroethoxy)phosphazene), PBFP

M. Kojima* and J. H. Magill†
Metallurgical and Materials Engineering Department, School of Engineering, Pittsburgh, PA 15261, USA
(Received 14 February 1985; revised 4 July 1985)

Spherulite formation in poly(bis(trifluoroethoxy)phosphazene) has been investigated from the melt and from solution over a relatively wide crystallization and annealing range. Three polymorphic forms and one meso-form is found in this polymer. Several of these crystal modifications coexist in amounts which depend upon the crystallization conditions. Negatively birefringent spherulites increase in birefringence slightly upon being heated through the thermotropic $T(1)$ transition. This change involves the formation of a chain extended morphology from a chain folded one. Microbeam X-ray analysis made within the spherulite shows that the unit cell [a] direction is along the spherulite radius while the [c] chain direction lies transverse to the spherulite radius. Moreover, below $T(1)$ it has been established that the X-ray long period is invariant with annealing time and temperature, and above $T(1)$ the periodicity disappears, or cannot be recorded. Whenever heating or cooling occurs through $T(1)$, the spherulite birefringence appears to be invariant after initially heating through $T(1)$. However, a substantial volume change (by dilatomery) of 6% occurs through $T(1)$ and this is consistent with a change in crystal structure from a 3D orthorhombic structure below, to a 2D hexagonal form above $T(1)$. From the molten state the transformation occurs rapidly from isotropic to the 2D form of the mesostate, not far below T_m. The 2D hexagonal form reverts to 3D chain extended orthorhombic on cooling below $T(1)$. This stable chain extended morphology also arises whenever PBFP is melted and then cooled below $T(1)$. All transformations from the isotropic melt or the folded chain conformation must pass through the mesophase. All specimens are friable upon cooling below $T(1)$, whereas the solution case spherulitic polymer film is ductile here.

(Keywords: poly(bis(trifluoroethoxy)phosphazene); melt-grown spherulites; solution grown spherulites; crystal orientation; structural modifications; crystallite sizes and lamellae)

INTRODUCTION

Stokes[1] first synthesized a chlorophosphazene rubber in 1897, but linear high molecular weight polymers were only made[2] for the first time in the mid 1960s. Since this time many polyphosphazenes have been prepared[3]. The semi-crystalline nature of linear hompolymers of this kind have been well established and their ability to undergo a mesomorphic transition is now documented in several publications[4-7]. However, the precise structures formed at and below the $T(1)$ transition have not been well established. Similarly the spherulitic morphology[4], though well recognized from relatively concentrated polymer solutions, requires further examination. Needle-like aggregates (not spherulites) in PBFP have been reported but detailed morphological information with crystallization conditions is scarce. Literature reviews[8-11] have provided good 'state of the art' perspectives on polyphosphazenes. Some of the current open questions or problems have been highlighted in these articles.

Recently, investigations (published[12,13] and in press[14]) have attempted to examine and to clarify some of the structural features of polyphosphazenes. Solution grown crystals have been reported[12,13] and some crystalline modifications elucidated. Mechanical behaviour (creep[14] and dynamic moduli[15]) have been investigated while orientation and density[15], ageing[14] and thermal stability[16] have received some attention. The purpose of the present paper is to document and extend some earlier reports from our laboratory[17], particularly on the spherulitic crystallization of PBFP polymer thin films. Textural and structural changes after treatment have been examined, principally by X-ray diffraction, scanning and transmission electron microscopy and optical microscopy. The coexistence of diverse crystal modifications and morphologies (for PBFP solidification conditions) is summarized briefly in the form of a phase diagram. The polymorphic complexities of PBFP have caused problems in crystal structure analysis. Progress has been vexingly slow, presumably because of the polymorphism highlighted here and elsewhere[12,13].

At present, the authors are aware of only two published crystal structures, one for poly(dichlorophosphazene)[18] and the other for poly(di-3,4 methyl-phenoxy-phosphazene), respectively[19]. Using epitaxial polymerization[20] however, halogenated polyphosphazene single crystals have lately been prepared and characterized.

The $T(1)$ transition in crystalline polyphosphazenes sets an upper limit in the load bearing applications of certain polyphosphazenes. Even so, applications[21,22] of polyphosphazenes continue to grow despite material costs which are high at present.

* Permanent address: Chisso Corporation, 2-7-3 Marunouchi, Chiyoda-ku, Tokyo, Japan.
† Also affiliated with Department of Chemical/Petroleum Engineering.

EXPERIMENTAL

Materials

Poly(bis(trifluoroethoxy)phosphazene) samples were kindly provided by Professor H. Allcock and Drs G. Hagnauer and R. Singler of the Army Materials and Mechanics Research Center for samples synthesized[2] by thermal melt polymerization of the cyclic hexachlorotrimer to produce the poly(bisdichlorophosphazene) which was then converted by nucleophilic substitution into the organosubstituted PBFP polymer. The polydispersity of these polyphosphazenes is typically $M_w/M_n \geqslant 10$.

Spherulitic film preparations

Several preparative procedures were employed for making spherulitic polymer films namely: (i) by casting spherulitic films from THF (0.1 at. wt% polymer approximately) on glass followed by slow solvent evaporation; (ii) films were also cast on a clean water surface and the solvent allowed to evaporate at room temperature. Thin films produced in this way were transferred onto carbon coated microscope grids and examined by TEM. Samples were also heat-treated (isothermally) above as well as below $T(1)$ to bring about morphological changes. Some thin film samples were also melted above T_m and then crystallized at temperatures above, as well as below $T(1)$.

Melt-crystallized specimens were prepared between glass cover slips in thermostatically-controlled silicone oil baths after the polymer was fused at 250°C for 5 min. Except for specimens prepared in this manner all other sample annealings (with free film surfaces) were conducted under nitrogen to avoid or minimize degradation. Even though the transfer of molten specimens from melt to the crystallization bath(s) was less than one second PBFP could not be quenched to the glassy state.

X-ray diffraction measurements

PBFP films were examined using: (i) Philips-microbeam camera and (ii) Statton (flat) vacuum camera with heater and temperature control accessories. Cu Kα radiation was employed in both instances. Small-angle X-ray measurements were made with a Rigaku–Denki camera and a 6 kW Rotating Anode using Cu Kα radiation.

Microscopy

Electron microscopy. Thin films were studied in the transmission and diffraction at 120 kV using a JEOL JEM-100U electron microscope. Samples were sometimes shadowed with Pd/Au (40/60 alloy) to enhance imaging.

Scanning electron microscopy. A JEOL JSM-35F scanning electron microscope was used to study cast polymeric PBFP surfaces coated with Au metal.

Optical microscopy. Crystallized polymer films were examined with a Leitz Ortholux research microscope fitted with a Mettler Hotstage and 35 mm Leitz camera. Birefringence measurements were made with a Berek compensator using polarized green light.

RESULTS AND DISCUSSION

Morphology of solution cast films

Uniformly thick PBFP films prepared at room temperature, were composed of negatively birefringent spherulites (see *Figure 1*). Microbeam X-ray diffraction measurements made with a 30 μm diameter X-ray beam, on spherulites 200 μm diameter, revealed that the structure was orthorhombic with the [*a*] growth direction lying along the spherulite radius direction (arrowed). The X-ray diffraction pattern insert in *Figure 1* (radial direction arrowed) shows the orientation. Indexing of the diffraction pattern was carried out using a well drawn spherulitic PBFP fibre (× 10 draw ratio) oriented just below $T(1)$, to give a [*c*] axis repeat distance of 4.86 Å (d_{001}). The other unit cell dimensions were determined as $a = 10.16$ Å and $b = 9.35$ Å from the diffraction insert, and the structure was designated α-orthorhombic.

Spherulites with free surfaces (see *Figure 2*) were examined by scanning electron microscopy and they had a fibrillar texture. The electron micrograph of the spherulitic fibrillar morphology (in *Figure 3*) was obtained from a thin film shadowed with Pd/Au (40/60 alloy). Similar surface features were found in thicker samples such as *Figure 2* using replication methods. The intermeshing fibrils (best illustrated however in *Figure 3*) splay and branch for space filling reasons, but their growth direction is still relatively well defined. From the diffraction pattern symmetry (*Figure 3*) the crystallites comprising the fibrils

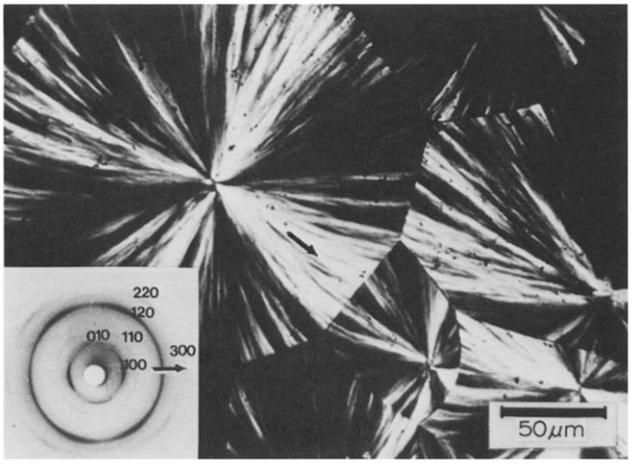

Figure 1 Typical PBFP negatively birefringent spherulites crystallized from THF solution at room temperature. The insert illustrates an indexed microbeam X-ray diffraction pattern in which the crystallographic [*a*] axis direction is parallel to the spherulite radius. Orientation directions within spherulite and diffractions pattern are arrowed

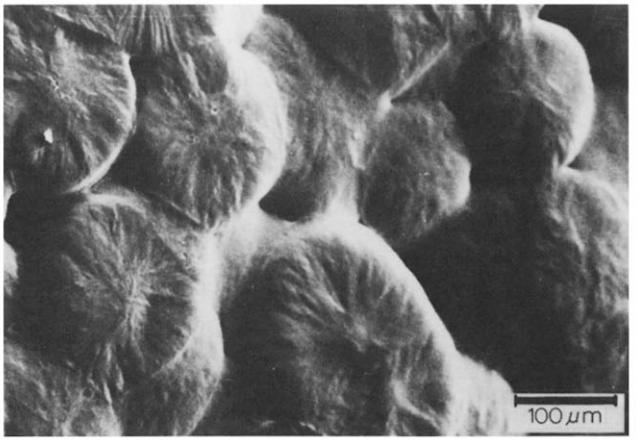

Figure 2 Scanning electron micrograph of PBFP spherulites cast from the concentration THF solution at room temperature. Specimens were sputtered with Au in an argon atmosphere at 10^{-2} Torr. Micrograph was taken at 15 Kv

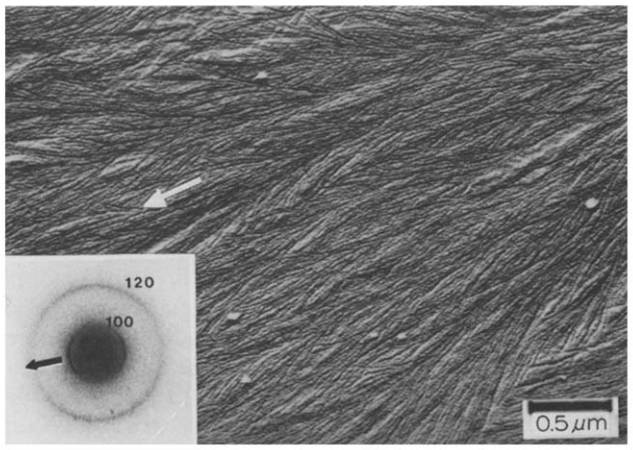

Figure 3 Electron micrograph of a solution cast thin PBFP spherulite, after it was shadowed with Pd/Au alloy 40/60 (w/w) composition. The indexed diffraction pattern insert obtained from a thin unshadowed film of this same PBFP specimen indicates that an orientation corresponding to the microbeam X-ray diffraction pattern in *Figure 1*. Growth directions arrowed in both diagrams

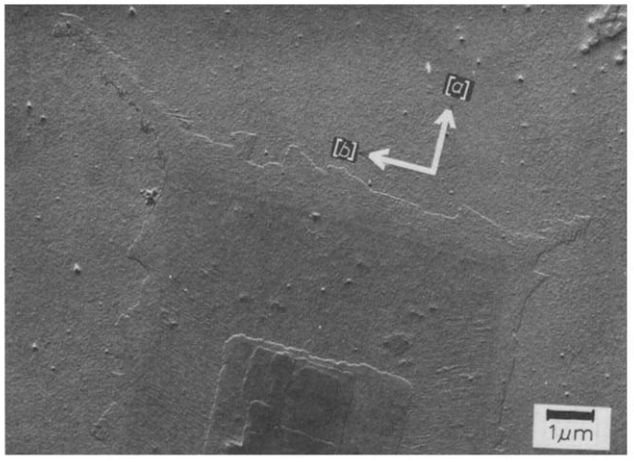

Figure 4 Electron micrograph of solution grown crystals of PBFP crystallized from 0.03 wt% polymer in 50/50 (v/v) THF/xylene. The [*a*] direction corresponds to the long axis of the crystal and [*b*] is perpendicular to it. Besides, these directions parallel the dendrite-like fibrillar growth formed in the [110] directions at the top right and left corners of the thinner crystal platelets. Note also the presence of surface striations in the crystals parallel to [*a*] and [*b*], respectively

must twist in a non-cooperative manner as they grow almost radially from the spherulitic centre, since the spherulites are not ringed. Fibrillar looking crystals are also seen to emerge from the crystal corners (upper right and left regions in the micrograph, in *Figure 4*). On the surface of the crystal, striations or overgrowths are arranged parallel to the [*a*] and [*b*] crystallographic axis directions, respectively. The more rapid growth takes place in the [110] direction at the crystal tips. The rather ragged looking (100) and (010) surfaces are probably a consequence of the solvent system used since texture and solvent compatibility are interrelated. A much clearer picture of the mergent fibrillar texture is shown in *Figure 5*. Here again, the [*a*] and [*b*] axis directions (arrowed) correspond to equivalent growth patterns depicted previously. Note that the same PBFP crystal morphology is found for crystals prepared by the conventional dilute solution crystal preparation procedure or in the dynamic crystal retraction method (DCRM) described elsewhere[14]. In the latter technique, thin polymer films of well defined crystals are grown on a carbon coated glass microscope slide which was slowly retracted (1 mm/h) from a solution of PBFP in THF or other solvents. Growth pattern correlations between spherulite and single crystal morphologies have now been clearly established. The [*a*] direction corresponds to the longer crystal axis (arrowed) and the slower transverse growth, [*b*] direction, is transverse to it.

Overall, a consistent morphological pattern exists for the solution grown spherulites, where for the first time in polyphosphazene materials, both electron and small-angle X-ray diffraction including wide-angle microbeam X-ray diffraction have been carried out on the same materials.

The X-ray diffraction patterns of a highly drawn PBFP fibre is shown in *Figure 6*. An α-orthorhombic structure with unit cell dimensions corresponding to $a=10.16$ Å, $b=9.35$ Å, $c=4.86$ Å was deduced so that in *Figure 6* the c spacing corresponds to a single monomer repeat unit. Along the equatorial direction, a weak doublet is associated with the (110) reflection of the α-orthorhombic modification. This reflection indexes as the $(\bar{1}10)$ in *Figure 6a*, and is assigned to a monoclinic modification, recently noted by us using electron microscopy as the β-modification[12] of PBFP. It was obtained from the dilute solution crystallization of low molecular weight PBFP.

Whenever PBFP is moulded and well-stretched above $T(1)$, say at 120°C, the highly oriented structure (*Figure 6b*) is maintained during cooling to room temperature. The unit cell dimensions are, as $a=20.6$ Å, $b=9.40$ Å and $c=4.86$ Å (and this is assigned as γ-orthorhombic). The α-orthorhombic cell has 2 monomer units and the γ-cell contains four monomer units. The crystallinity appears to be less than it is in the γ-modification where the reflections are sharper and the background clearer, but quantitative X-ray crystallinity measurements are now in progress to obtain the degree of crystallinity for variously prepared samples[23].

The small-angle X-ray spacing for as cast PBFP (spherulitic) films is difficult to measure, but a well defined discrete reflection (<200) appears after annealing before $T(1)$ at 70°C, for example. This spacing is much larger

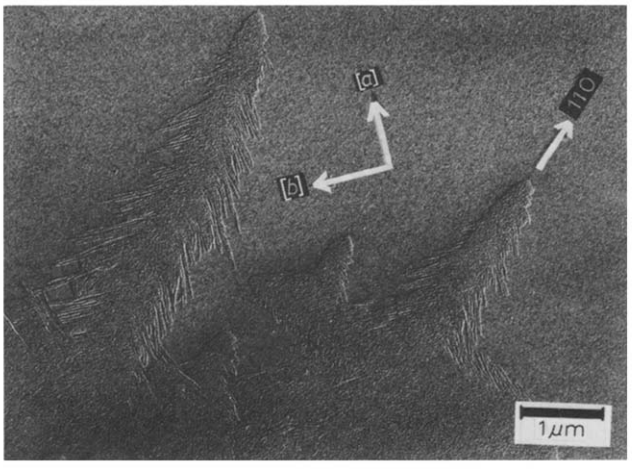

Figure 5 Electron micrograph of higher magnification solution grown PBFP crystal prepared in the same manner as *Figure 4*. Note growth directions [*a*] and [*b*] correspond the arrow markings. The fast growth [110] is arrowed too. The [*c*] chain direction is perpendicular to the *a*–*b* basal plane

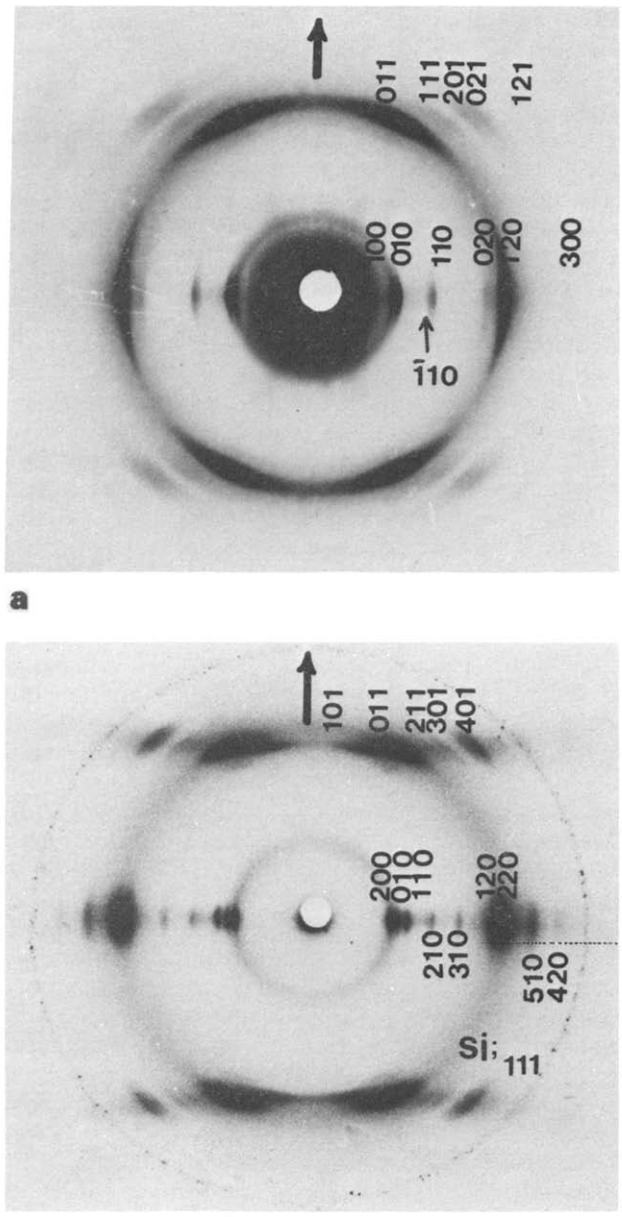

Figure 6 (a) X-ray diffraction pattern by Cu Kα radiation obtained from a PBFP film (stretched × 10). The fibre axis is vertical (arrowed). The indexed structure is α-orthorhombic modification with unit cell dimensions of $a=10.16$ Å, $b=9.35$ Å and $c=4.86$ Å. Note a faint diffraction doublet (arrowed) which indexes as ($\bar{1}10$) corresponding to the β-monoclinic modification. (b) X-ray diffraction pattern by Cu Kα radiation of a PBFP samples stretched at 120°C (above $T(1)$). Fibre axis vertical. The indexed γ-orthorhombic modification has dimensions $a=10.6$ Å, $b=9.40$ Å and $c=4.86$ Å

than the average 156 Å dimension obtained for single crystal mats which were also cast or annealed below $T(1)$. The disappearance of a discrete small-angle peak, at or above $T(1)$ (*Figure 7*) supports other morphological work[14] on single crystals heated through this transition temperature. Clearly, these measurements indicate that the small-angle periodicity in spherulitic samples is larger than it is in single crystals also formed below $T(1)$. This result is not unexpected since the low-angle periodicity obtained for single crystal mats is invariably less than the value found in bulk homopolymers crystallized at the same temperature.

Annealed morphologies and phase transitions

The dilatometric curves (*Figure 8*) depict the volume changes and phase transformations in PBFP after it has been heated once through $T(1)$ and cooled. Correspondingly, some diffraction pattern inserts in *Figure 9* (with the exception of *Figure 9a* which refers to the chain-folded α-form* from THF solution) are indicated by lettered inserts (*Figure 8*) at several temperatures. The volume–temperature, morphology relationships are therefore illustrated below $T(1)$ for an γ-orthorhombic structure and through $T(1)$, where it changes to a 2D hexagonal modification, which is also chain extended† and a more open structure. The mean separation between molecular chain centres is estimated at 10.16 Å approximately from diffraction measurements. The polymer density and hence

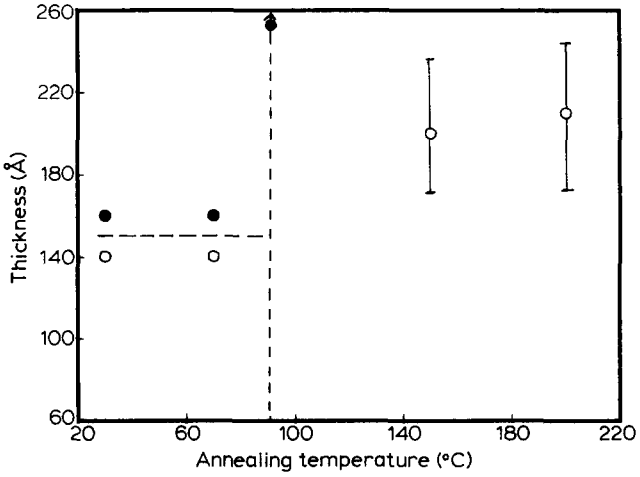

Figure 7 Small-angle X-ray scattering[13] from samples prepared below and above $T(1)$: open circles TEM; closed circles SAXS (crystals)

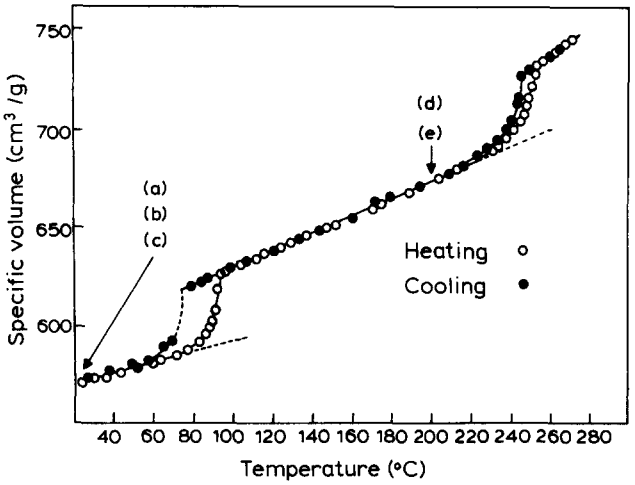

Figure 8 Dilatometric PBFP heating (open circles) and cooling (closed circles) curves as function of temperature over the crystallization area of interest. Lettered regions of the diagram correspond to annealing or heat treatment conditions cited for some selected morphological studies reported here. The designations are: (a) original solution cast PBFP spherulitic film (chain-folded); (b) specimen (a) after heating to 200°C (chain-extended, 2D); (c) specimen (a) after melting at 250°C (amorphous); (d) denotes sample heated from room temperature to 200°C (chain extended, 2D); (e) denotes specimen cooled to 200°C from the melt at 250°C (chain extended, 2D). See ref. 14

* This form, well documented elsewhere[13], passes directly and irreversibly into the γ-form after it is heated above $T(1)$ and cooled down again (*Figure 10*, schematic pattern).

† Chain extended is used reservedly here for a significant but unknown degree of extension, contrasting with the term extended chain commonly used to depict a fully extended molecular morphology.

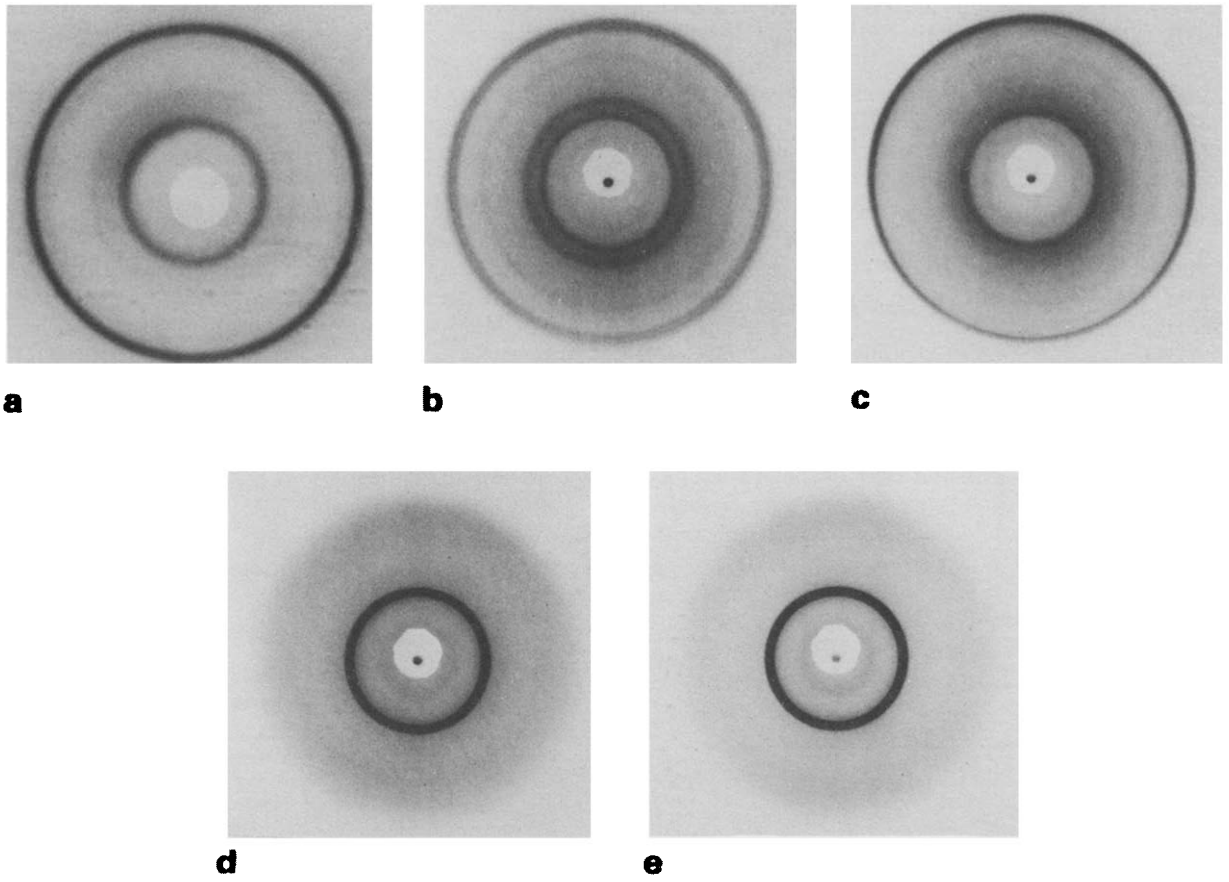

Figure 9 X-ray diffraction patterns of heat treated PBFP spherulitic film corresponding to circumstances depicted in *Figure 8*

crystallinity again decreases substantially on passing from below $T(1)$ upwards through T_m into the molten state. A volume change of more than 12% is encountered in this overall excursion, i.e. approximately 6% at each of the first order transitions $T(1)$ and T_m, plus the expansion which occurs in the region between $T(1)$ and T_m. This may be estimated from data in *Table 1*. Incidentally, dilatometry unambiguously defines the nature of these thermodynamic transitions much better than the d.s.c. technique.

Expansion coefficients determined in this work for PBFP along with literature data, are given in *Table 1*.

This form, well documented elsewhere[13], passes directly and irreversibly into the γ-form after it is heated above $T(1)$ and cooled down again (*Figure 10* schematic pattern).

Mesophase diffraction

A unique morphology is depicted within the diffraction ring pattern of *Figure 11* which is an enlargement from *Figures 9d* or *9e*, for example. However, it does appear in all diffraction patterns taken in the mesophase temperature range. In *Figure 11a* and its insert *Figure 11b*, sets of arcs are disposed hexagonally within the relatively broad (100) reflection of the 2D hexagonal phase. The same diffraction patterns are obtained in the $T(1)$ to T_m interval, independent of the manner of getting there (reaction path).

Figure 11c contains a processed digital scan* across the diffraction ring (*Figure 11a*) where the inner arcs are now more clearly illustrated. From the peak half widths, using the Scherrer formula†, $t = K/B\cos\theta$, it is estimated that the domain dimensions are typically 1500 to 2000 Å, in the thermotropic region. These dimensions are supported by recently observed morphologies[24] which are obtained whenever specimens are crystallized from the 2D phase and then cooled quickly into the 3D state for inspection at room temperature. The suggestion here is that from $T(1)$ to just below T_m, chain-extended precursors for the 3D (γ'-orthorhombic) phase exist and that these crystallize three dimensionally with a decrease in volume of 6%, and concomitant ordering in the chain direction. The spacings of the reflections (*Table 2*) in the mesophase (see for example *Figure 11a* and *b*) are tabulated at two temperatures, one near $T(1)$ and the other not too far below T_m.

Table 1 Linear expansion coefficients, α, for PBFP

Sample form	Temperature range	This work (α)	Literature (α)
Cast film	100°C–200°C	1.7×10^{-4}	1.8×10^{-4} [25]
Melt film	100°C–200°C	2.7×10^{-5}	
Molded film			2.5×10^{-4} [25]
Dilatometry (linear value)			2.33×10^{-4} [13]

A mean coefficient of linear expansion ($\alpha = 2.6 \times 10^{-4}$) was calculated from these and other X-ray dimensions obtained between 100°C and 200°C that is in good agreement with other values[25] obtained for moulded specimens[13], but it is greater than the value found from

* Obtained by Dr Todhunter in the Pattern Recognition Laboratory of the Electrical Engineering Department, University of Pittsburgh.

† In this equation t is associated with mesophase clusters or crystallite size, K is a parameter presumed to be 0.9, λ is the Cu Kα wavelength of 1.542 Å, θ is the Bragg angle, and B the profile width of the sharp inner reflections.

cast spherulitic films. These trends are to be expected. The (α) value for film and moulded materials are comparable. Both specimens must contain some disordered material* probably created by the reorganizational process associated with crystal thickening when heating is carried out through $T(1)$. In dilatometry[13], the expansion coefficient appears to be larger because some amorphous or disordered polymer must be present in the relatively large 1.5g sample used in these measurements. Crystallinity determinations below $T(1)$, using the X-ray technique, are being made on variously prepared specimens.

The $T(1)$ morphology

Creep[14] and dynamical mechanical measurement[7,15] on PBFP indicate that in the 2D mesophase range the properties are considerably softer than in the 3D crystalline state below $T(1)$. For this reason the term 'viscous crystalline structure'[26] has been used to describe this 'soft' condition in some other polymeric systems too.

Prolonged annealing or heat cycling of the sample(s) through the $T(1)$ transition and back to room temperature again for numerous cycling times (10–30), results in an enhancement in the $T(1)$ heat of fusion of some 35% compared with a solution cast spherulitic sample with an enthalpy of about 6.5 cal/g. This significant increase in heat content must be associated with improved packing or ordering of the mesophase morphology from the 2D pseudohexagonal arrangement, ostensibly into the 3D γ-orthorhombic crystals which form upon cooling below $T(1)$.

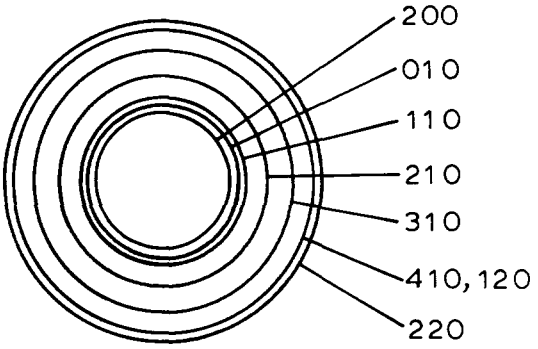

Figure 10 X-ray diffraction pattern obtained after heating above $T(1)$ 250°C and cooling down to room temperature again. The PBFP phase is indexed in the diagram

*Recent morphological evidence from electron micrographs of thin films of PBFP supports this statement.

When solution cast negatively birefringent spherulites are heated through $T(1)$ a small change (increase) in birefringence occurs. This change is associated with an invariant [a] axis orientation as the structure changes from 3D α-orthorhombic to 2D pseudohexagonal†. Whenever this transformation occurs further heating or cycling does not alter significantly the birefringence, even though the results in *Figure 8* clearly show that a less dense phase exists above $T(1)$. On both sides of $T(1)$ a chain extended morphology exists after the initial passage through $T(1)$. Above $T(1)$ there is disorder along the chain direction due to the mobility of the $-OCH_2CF_3$ side groups[5]; below this transition the 3D, γ-orthorhombic form exists.

Spherulites and aggregates grown from the melt

Spherulitic and other morphological habits obtained after crystallizing thin films of molten PBFP (between glass coverslips) are diverse and numerous even within

†The initial volume change from α-orthorhombic to 2D hexagonal has not been measured by dilatometry because of experimental difficulties, however d.s.c. measurements have indicated enhancement of $T(1)$ by 20°C or more after the first run.

Table 2 Diffraction from the mesophase[a]

	d spacing in Angstroms at	
Line	100°C	200°C
1 (Outer edge)	11.0	11.3
2 (inner sharp reflections)	10.5	10.8
3 (inner sharp reflections)	10.1	10.4
4 (inner edge)	9.7	9.9

[a] The broad outer (second) ring in the hexagonal modification noted by us and also reported elsewhere[25], is not seen in our patterns (measured at room temperature) because our camera geometry limits our recording it.

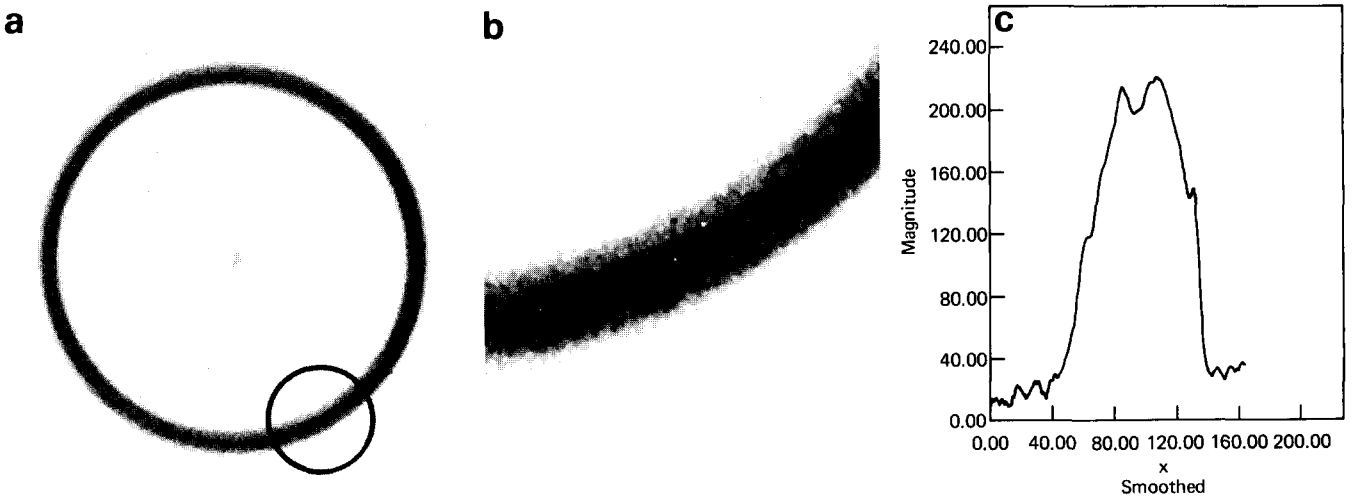

Figure 11 (a) X-ray diffraction pattern of the (100) reflection for PBFP at 200°C. This represents an enlarged version of *Figure 9* to reveal fine features found within the (100) pseudohexagonal ring. (b) Note the hexagonal disposition of very sharp lines within the ring. These arcs originate from the hexagonal mesomorphic morphology. (c) Computer scan of the arcs within the broad (100) ring

the same sample cooled over a moderate crystallization range (225°C–235°C approximately). Morphological forms are more varied and even less controllable in PBFP than in polyamides where many forms have been obtained[27]. *Figures 12* and *13* contain some examples of these PBFP morphologies. Melt crystallized negatively birefringent spherulites, crystalline aggregates, and other well-oriented needle-like structures occur. Relatively large

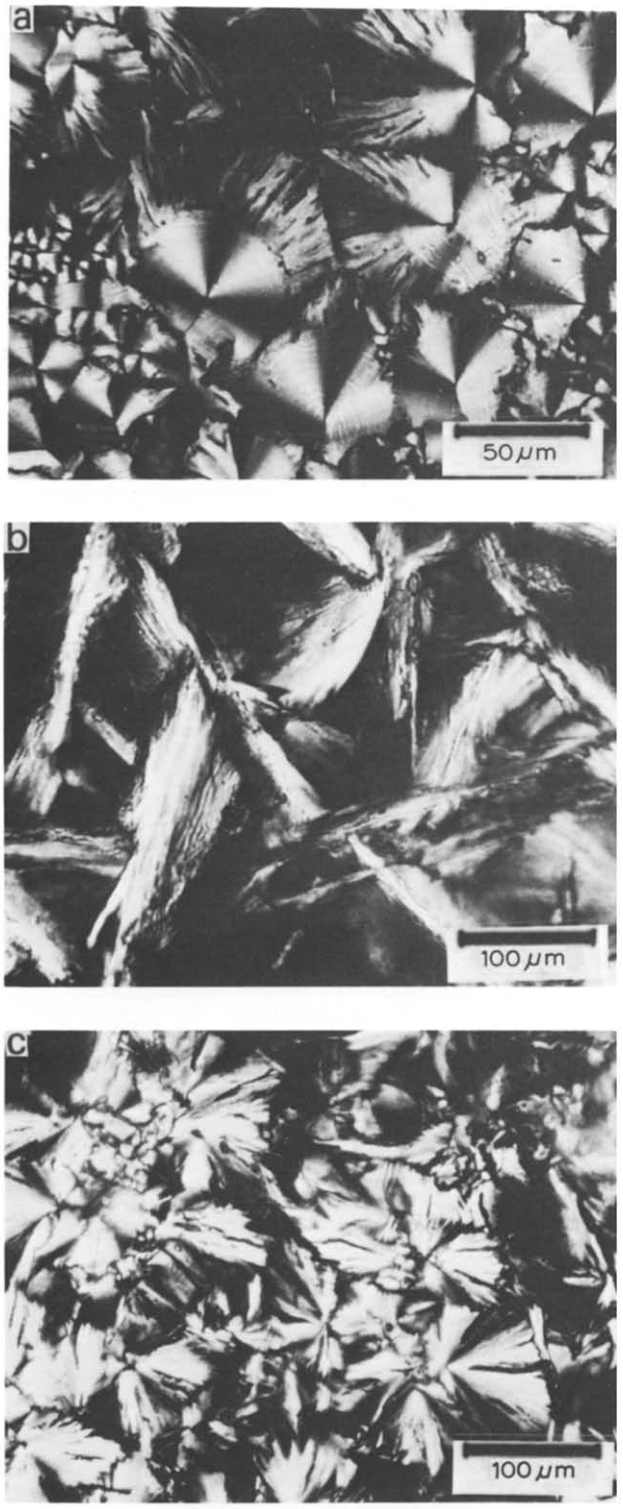

Figure 12 Morphological forms obtained after melting PBFP at 250°C (5 min) followed by isothermal crystallization at 231°C, quenching in liquid nitrogen and then reheating to room temperature. Some illustrated morphologies are: (a) negatively birefringent spherulites; (b) aggregated crystals); (c) crystalline spherulitic aggregates

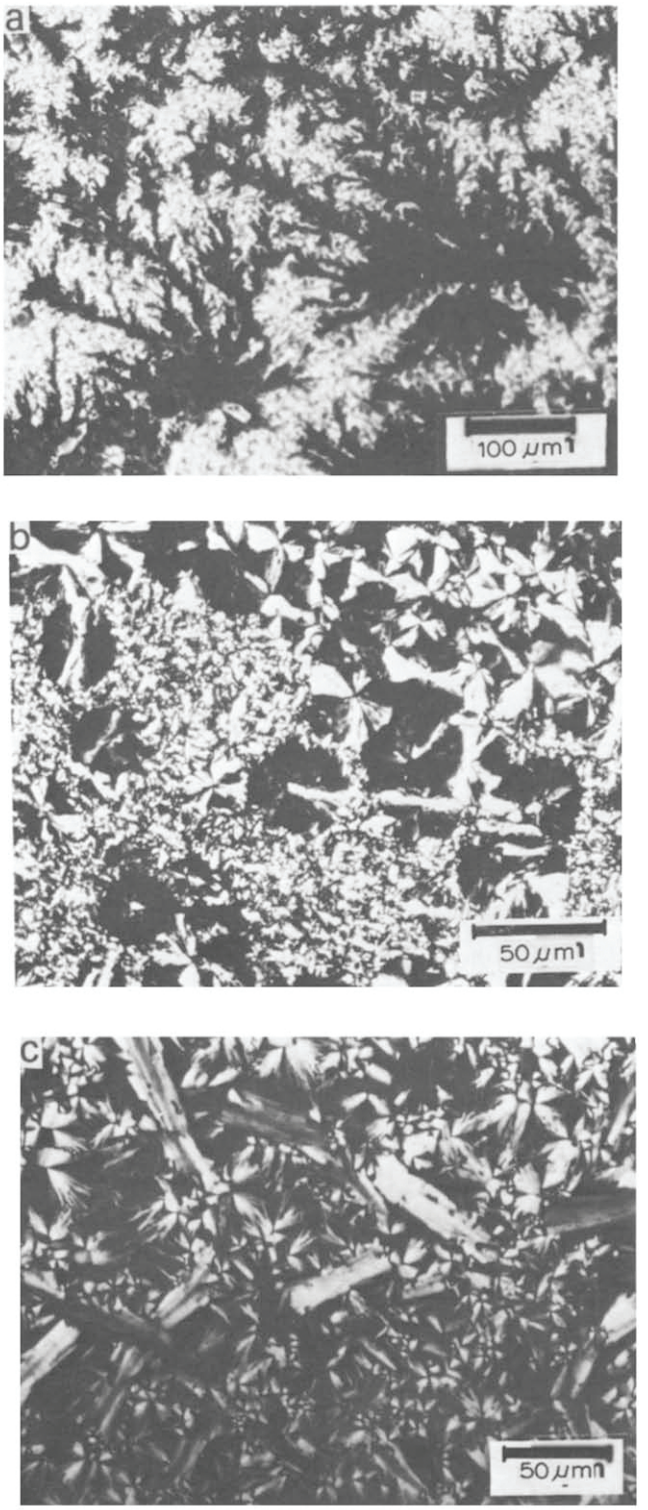

Figure 13 Typical crystalline textures found in isothermally crystallized films at 224°C, after quenching to dry ice temperature, −70°C, and returning to room temperature when some selected structures are: (a) dendritic aggregates of very low birefringence; (b) zero birefringent spherulites; (c) spline-like crystals, amongst other needle-like morphologies

well-ordered birefringent rod-like structures are also formed as well as other birefringent moieties ranging from essentially dark dendritic morphologies and almost zero birefringent spherulites, to more highly birefringent spline-like crystals observed at room temperature. Optical micrographs of solution grown negatively birefringent spherulites and needle-like non-spherulite structures have been mentioned[4] elsewhere.

The diverse optical forms highlighted in this preliminary work are complex and require detailed examination by many techniques. Several authors[28–30] have indicated that the organization of macromolecular mesophases is still ambiguous and cannot be settled by optical microscopy alone. The scale of texture of microstructures often lies beyond to resolution limit of the optical microscope and even some X-ray techniques. The bright and dark field electron microscope is now proving useful for the characterization of polyphosphazenes[31].

CONCLUSIONS

(1) Negatively birefringent PBFP fibrillar spherulites are formed from solution. The crystallite [a] axis direction lies predominately along the spherulite radius with [c] and [b] axes directions essentially transverse but twisting non-cooperatively around it.

(2) Solution cast spherulites undergo a transition when first heated above $T(1)$. Their birefringence becomes more negative but then finally decreases to zero whenever melting occurs. In this sequence of events the unit cell (a 3D chain-folded α-orthorhombic modification) transforms to a 2D chain extended pseudohexagonal modification. Upon cooling the specimen below $T(1)$, it changes to a γ-orthorhombic 3D chain extended modification which is now more stable than the original α-modification.

(3) The [a] axis of the spherulite and the long axis of solution grown orthorhombic crystals have a common growth direction.

(4) The unit cell dimensions of the 'chain folded' α-modification are $a=10.16$ Å, $b=9.35$ Å and $c=4.86$ Å. In stretched solution cast spherulitic films, a trace of a new phase, termed a β-monoclinic modification, coexists with the α-orthorhombic modification whenever low molecular weight PBFP is used. In spherulitic films, stretched above $T(1)$ and cooled again, the γ-orthorhombic unit cell is larger with dimensions $a=20.6$ Å, $b=9.40$ Å and $c=4.86$ Å. Above $T(1)$ only a chain-extended 2D pseudohexagonal thermotropic phase is present.

(5) Solution cast PBFP films and single crystal mats exhibit a discrete X-ray long period below $T(1)$, but not above it.

(6) Transformations through the $T(1)$ region are reversible for volume, but are essentially birefringent invariant after the first pass through this region. The chain folded (α) to chain extended (γ) orthorhombic modification, must always pass via the 2D mesophase phase. A lamellar morphology is only obtained when the polymer is crystallized from solution.

(7) In the mesophase region, from the width of the sharp hexagonally arranged area found within the broad (100) ring, it is estimated that domain dimensions of 1000–2000 Å are present; assessed from X-ray diffraction, and now confirmed recently[24] by electron microscopy.

ACKNOWLEDGEMENTS

The authors are indebted to the National Science Foundation (Polymers Program) for supporting this research in part.

REFERENCES

1 Storkes, H. N. *J. Am. Chem. Soc.* 1897, **19**, 782
2 Allcock, H. R., Klugel, K. L. and Valen, K. L. *J. Inorgan. Chem.* 1966, **5**, 1709
3 Allcock, H. R. *Polym. Chem. Sci., Prog. Oxford* 1980, **66**, 355
4 Schneider, N. S., Desper, C. R. and Singler, R. E. *J. Appl. Polym. Sci.* 1976, **20**, 3087
5 Alexander, M. N., Desper, C. R., Sagalyn, P. L. and Schneider, N. S. *Macromolecules* 1977, **10**, 721
6 Desper, C. R. and Schneider, N. S. *Macromolecules* 1976, **9**, 424
7 Allen, G. and Morten, R. M. *Polymer* 1972, **13**, 253
8 Korsak, V. V., Vinogradova, S. V., Tur, D. R., Kasarova, N. N. Komarova, L. I. and Gilman, L. M. *Acta Polym.* 1979, **30**, 245
9 Schneider, N. S., Desper, C. R. and Beres, J. J. 'Mesomorphic Structure in Polyphosphazenes' in Liquid Crystalline Order in Polymer, Ch. 9, pp. 229–325, Academic Press, New York, (1978)
10 Allcock, H. R. *Angew Chem. Int. Ed. Engl.* 1977, **16**, 147
11 Tate, D. P. *J. Polym. Sci., Polym. Symp. Edn.* 1974, **48**, 33
12 Kojima, M. and Magill, J. H. *Polymer* 1983, **24** (*Commun.*), 329
13 Kojima, M., Kluge, W. and Magill, J. H. *Macromolecules* 1984, **17**, 1421
14 Masuko, T., Simeone, R. L., Magill, J. H. and Plazek, D. J. *Macromolecules* 1984, **17**, 2857
15 Choy, I. C. and Magill, J. H. *J. Polym. Sci. Polym. Chem. Edn.* 1981, **19**, 2495
16 Peddada, S. V. and Magill, J. H. *Macromolecules* 1983, **16**, 1258
17 Magill, J. H. 'Transitions in Polyphosphazene Homopolymers and Copolymers', Proceedings of the 11th Annual North American Thermal Analysis Meeting paper No. 65, p. 381, New Orleans, LA, USA, and Magill, J. H. 'Transition in Polyphosphazenes', Proceedings 12th Annual North American Thermal Analysis Meeting paper No. 51, p. 177, Williamsburg, VA, USA, 25–29 Sept. 1983
18 Allcock, H. R., Arcus, R. A. and Stroh, E. G. *Macromolecules* 1980, **13**, 919
19 Burkhart, C. W., Gillette, P. C. and Lando, J. B. *Bull. Am. Phys. Soc.* Dallas Meeting, Texas (1982) Abstract HR11, p. 322
20 Nae, N., Lando, J. B., Baer, E. and Richert, S. E. *Bull. Am. Phys. Soc.*, Dallas Meeting, Texas (1982), Abstract J49, p. 360
21 Gerber, A. H. *J. Am. Chem. Soc.* 1979, **41**, 81
22 Singler, R. E., Hagnauer, G. L. and Sicka, G. W., 'Elastomers and Rubber Elasticity', ACS Symposium Series, No. **193**, The American Chemical Society (1982), p. 229
23 Kojima, M., MacManus, G. and Magill, J. H. (unpublished work)
24 Kojima, M. and Magill, J. H. *Makromol. Chem.* 1984, **186**, 649
25 Desper, C. R., Beres, J. J. and Schneider, N. S. 'Mesomorphic Structure in Polyphosphazenes', IUPAC Symposium (1983), p. 682
26 Beatty, C. L. and Karasz, F. E. *J. Polym. Sci., Polym. Phys. Edn.* 1975, **13**, 971
27 See for example, Magill, J. H. *J. Polym. Sci. A-2*, 1971, **9**, 815
28 Krigbaum, W. R. and Watanabe, J. *Polymer* 1983, **24**, 1299
29 Thomas, E. L. and Wood, B. A. *Faraday Discuss. Chem. Soc.* 1985, **79**, paper 15
30 'Polymer Liquid Crystals' (Eds. A. Ciferri, W. R. Krigbaum and R. B. Meyer), Academic Press, New York and London (1982)
31 Magill, J. H., Petermann, J. and Rieck, U. *J. Colloid Polym. Sci.* (submitted July 1985)